Computational insights into the catalytic role of the base promoters in ester hydrogenation with homogeneous non-pincer-based Mn-P,N catalyst

Journal of Catalysis 363 (2018) 136–143

Contents lists available at ScienceDirect

Journal of Catalysis

journal homepage: www.elsevier.com/locate/jcat

Computational insights into the catalytic role of the base promoters in ester hydrogenation with homogeneous non-pincer-based Mn-P,N catalyst ☆

Chong Liu [a], Robbert van Putten [a], Pavel O. Kulyaev [b], Georgy A. Filonenko [a], Evgeny A. Pidko [a,b,*]

[a] Inorganic Systems Engineering Group, Department of Chemical Engineering, Faculty of Applied Sciences, Delft University of Technology, Van der Maasweg 9, 2629 HZ Delft, The Netherlands
[b] TheoMAT Group, ITMO University, Lomonosova 9, St. Petersburg 191002, Russia

ARTICLE INFO

Article history:
Received 27 February 2018
Revised 16 April 2018
Accepted 17 April 2018

Keywords:
Ester reduction
DFT calculations
Ab initio thermodynamic analysis
Catalyst deactivation
Homogeneous catalysis
Reaction mechanism
Multifunctional catalysis

ABSTRACT

The reaction mechanism of ester hydrogenation catalyzed by a bidentate aminophosphine ligated manganese catalyst was studied by DFT calculations. Particular emphasize was placed on the role of the alkoxide base additives. The presence of such basic promoters as KO^{t}Bu can improve the catalyst activity by lowering the activation barriers of H_2 dissociation as well as the hydrogenation step. The promoting effect of KO^{t}Bu on H_2 activation is much stronger than that of *tert*-butoxides with other alkali metals, which is crucial for the catalyst regeneration from the deactivated Mn-alkoxide species in the resting state.

1. Introduction

Catalytic reductions of carbonyl derivatives such as ketones, aldehydes, and carboxylic acid derivatives with molecular hydrogen have become a critical synthetic strategy towards the production of a broad scope of bulk and fine chemicals [1–5]. Attractively, catalytic processes employing gaseous H_2 as the reductant principally operate waste-free, and thus are inherently more atom-efficient and environmentally benign compared to the stoichiometric processes employing such reducing agents as lithium aluminium hydride and sodium borohydride currently dominating the pharmaceutical industry [1,6]. While catalytic systems for the reduction of carboxylic acid derivatives historically were based on noble metals [3] (e.g. Ru, Os, and Ir), in recent years attention has shifted towards development of early transition-metal based catalysts such as Fe [7,8], Co [9–11], and Mn [12–15].

Due to its high natural abundance and excellent biocompatibility, manganese is considered an attractive metal for fine-chemical and pharmaceutical applications as the low toxicity renders quantitative removal of catalytic residues superfluous. Consequently, increased focus of the scientific community has culminated in exceptionally rapid development of a series of highly active Mn-catalysts capable of efficiently reducing particularly challenging carbonyl substrates such as carboxylic acid esters and nitriles [12,13]. This tremendous progress was associated in part with the use of well-established pincer ligand platforms [8,16,17], rather than by the development of novel tailor-made ligands for the chemically distinct Mn(I) systems. This transition, however, does not account for the divergent chemical reactivity of Ru and Mn. The latter, for example differ in the relative stability of metal alkoxide complexes, which are experimentally observed and are often considered off-cycle resting states. Transition metal alkoxides may be considerably more stable than their catalytically active hydride counterparts, as was demonstrated by Gauvin and co-workers in a detailed mechanistic study of acceptorless dehydrogenative coupling (ADC) of alcohols – the microscopic reverse of ester hydrogenation [18].

The often disadvantageous stability of Mn-alkoxides has also been proposed by us [19]. We experimentally observed an unusual dependence of the extent of ester hydrogenation by the Mn catalyst containing bidentate aminophosphine ligand (Mn-P,N **1**) on the concentration of KO^{t}Bu base promoter (Scheme 1). This obser-

☆ This paper has been submitted as a contribution to a Thematic Issue on Mechanism of Molecular Catalysts edited by Kuiling Ding and Matthias Beller.

* Corresponding author at: Inorganic Systems Engineering Group, Department of Chemical Engineering, Faculty of Applied Sciences, Delft University of Technology, Van der Maasweg 9, 2629 HZ Delft, The Netherlands.
E-mail address: e.a.pidko@tudelft.nl (E.A. Pidko).

https://doi.org/10.1016/j.jcat.2018.04.018
0021-9517/

vation led to the proposal of catalyst inhibition by small alcohols formed upon hydrogenation of the ester substrate, ultimately leading to the formation of stable manganese alkoxides [19]. Analogous to the Ru-based systems studied in detail by the groups of Bergens [20] and Morris [21], we hypothesized that the base is required to reactivate the catalytically active hydride species through the base-assisted alkoxide elimination [19]. In conjunction with the large effect of base loading, we experimentally found a strong impact of both the chemical nature of the Lewis acidic alkali metal cation (K > Na ≫ Li) and the alkoxide fragment (O^{t}Bu > OEt ≫ OMe) of the basic promotor on the catalytic activity of **1**.

As a separate phenomenon, the Lewis acid promotion is known in homogeneous (de)hydrogenation catalysis [22,23]. Namely, Hartmann and Chen demonstrated experimentally that N—H substitution for N-LA (LA = Li^+, Na^+, K^+) in Noyori-type catalysts is a viable pathway that may assist catalysis by cleavage of molecular H_2 bound to the Ru center with the involvement of an alkoxide anion [22]. Subsequently Dub et al. concluded that the presence of such an O—H functionality (e.g. alcoholic products, protic solvents, traces of water) indeed could reduce hydrogen bond cleavage energies by as much as 40–80 kJ mol^{-1} [24]. Similarly, it was shown that coordination of potassium to the Ru-N moiety reduced H_2 cleavage barrier by ca. 40 kJ mol^{-1} [25]. As these detailed works, with few exceptions [26], mainly address noble metal catalyzed ketone hydrogenation, a little is known about the role of base promoters in Mn-catalyzed hydrogenation of esters. With the impact of the base promoter apparently being more critical for Mn catalysis [19] compared to other systems, we aimed here at formulating the rationale behind this effect.

In this work we present a detailed computational study of the mechanism of ester hydrogenation by manganese complexes with bidentate aminophosphine ligands. Particular emphasis is placed on the role of Lewis acid and alkoxide additives that were shown to profoundly impact the catalytic performance. In particular we analyze separately the role of the base at the stage of Mn-P,N complex preactivation and its promoting role within the catalytic cycle for ester hydrogenation (Scheme 2). The results presented not only allow to refine and extend the mechanistic picture postulated earlier for this system but also to create a basis for the discussion of the specific role of base promotors in hydrogenation catalysis by multifunctional catalyst systems.

2. Computational details

All density functional theory (DFT) calculations were performed using the hybrid PBE0 exchange-correlation functional [27] as implemented in Gaussian 09 D.01 program [28]. Our previous studies on homogeneously-catalyzed processes [29,30] have evidenced the high accuracy and predictive power of this methodology for various homogeneously-catalyzed reactions. A recent detailed computational analysis by Leitner and co-workers demonstrates that PBE0 provides the optimal performance in terms of the correctness of the representation of the electronic structure and reactivity on Mn-containing systems in varying oxidation states [31]. Geometry optimizations were performed with all-electron 6-31G(d) basis set for all atoms, and vibrational analysis was then carried out for all structures at the same level to identify the true nature of the stationary points. All structures corresponding to local minima showed no imaginary frequencies, while transition state (TS) structures were characterized by a single imaginary frequency corresponding to the expected reaction coordinate. Intrinsic reaction coordinate (IRC) approach was employed to examine the connectivity between the transition states and the corresponding minima. The electronic energies were refined by single-point calculations with 6-311+G(d) basis set on all atoms. Bulk solvent effects were accounted for by single-point polarizable continuum model (PCM) corrected at this level of theory using the gas-phase-optimized geometries (THF solvent, ε = 7.4257). The reaction (ΔE_{ZPE}) and activation energies ($\Delta E^{\ddagger}_{ZPE}$) reported in the manuscript were corrected for zero-point energy (ZPE) from the normal-mode frequency analysis. Standard reaction Gibbs free energies (ΔG_{THF}) and activation Gibbs free energies ($\Delta G^{\ddagger}_{THF}$) in THF solution were computed using the results of the normal-mode analysis within the ideal gas approximation at a pressure of 1 atm and temperature of 373 K. For species in solution, the entropic contribution arising from translational degrees of freedom was computed as 1/2 of that for the isolated gas-phase molecule [32,33].

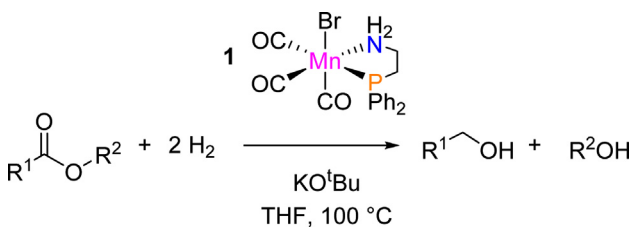

Scheme 1. Hydrogenation of ester with a Mn-P,N complex **1**.

3. Results and discussion

3.1. Pre-catalyst activation

The direct role of the base promotor in the catalytic ester hydrogenation with **1** and related halide transition metal complexes is to convert them to a catalytically active hydrido species **3** (Scheme 2) capable of sustaining the catalytic cycle. Fig. 1 presents the optimized structures for the reaction intermediates and transition states together with the computed energetics of the elementary reaction steps during the catalyst activation process. The corresponding free energy diagram is shown in Fig. 2. The first step in the catalyst activation sequence is the reaction of **1** with KO^{t}Bu base resulting in an exergonic exchange of the halide ligand in **1** with an O^{t}Bu group to form **2**. To enable the subsequent hydrogenolysis process, a coordination site on the Mn center needs to be liberated. This is achieved via a sequence of rather unfavorable reaction steps involving first the displacement of the O^{t}Bu ligand, which according to the current DFT calculations is accompanied by the deprotonation of the amino-moiety of the bidentate P,N ligand forming **2a** featuring a coordinated HO^{t}Bu molecule. This is followed by the displacement of HO^{t}Bu with an H_2 molecule to form a σ-complex **2c**. The complete reaction sequence is endergonic by 78 kJ mol^{-1} and proceeds with an apparent free energy barrier of 86 kJ mol^{-1} ($\Delta G°_{373K,THF}$; $\Delta G^{\#}_{373K,THF}$). Clearly, the rather weak coordination of molecular H_2 is not sufficient to compensate for the energy losses related to the deprotonation of the P,N ligand and the dissociation of the Mn-O bond during this transformation of the precatalyst **1** to intermediate **2c**. This reaction sequence can therefore be viewed as a pre-activation of both the Mn complex that is followed by a highly exergonic ($\Delta G°_{373K,THF}$ = −112 kJ mol^{-1}) and nearly barrierless ($\Delta E^{\ddagger}$ = 0 kJ mol^{-1}; $\Delta G^{\ddagger}_{373K,THF}$ = 10 kJ mol^{-1}) heterolytic splitting of the pre-coordinated H_2 via a 6-membered ring cyclic **TS$_{2c\text{-}2d}$** to give the Mn-hydrido adduct coordinated to HO^{t}Bu molecule (**2d**). The latter is leaving the reactive ensemble exergonically ($\Delta G°_{373K,THF}$ = −18 kJ mol^{-1}) to yield the octahedral complex **3**. The presence of the tert-butanol molecule in the second coordination sphere of Mn is crucial for this activation reaction sequence. First of all, the hydrogen bonding of an alcohol with the amido-motiety in the deprotonated trigonal-bipyramidal Mn-P,N complex (**2b**)

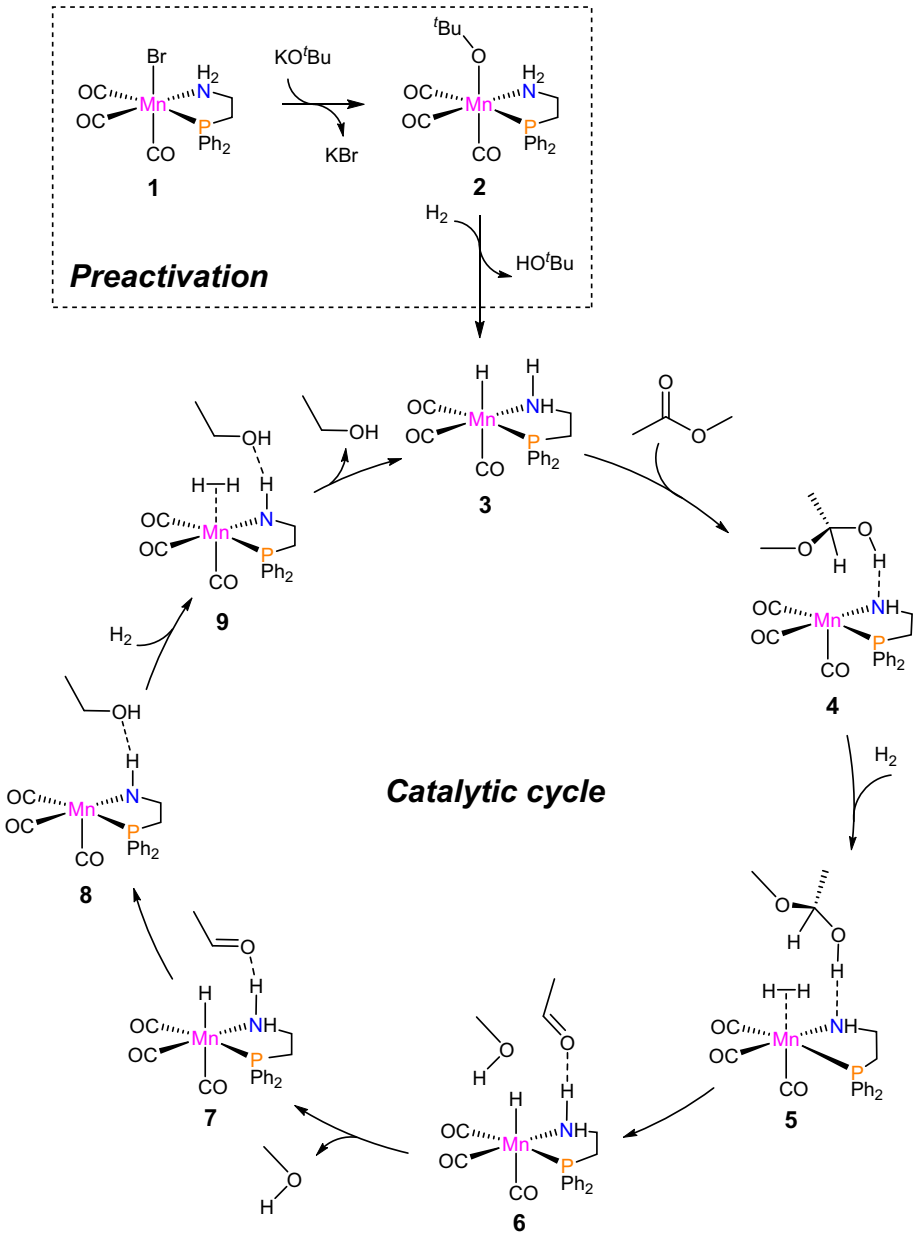

Scheme 2. Proposed reaction mechanism of ester hydrogenation catalyzed by Mn complexes [19].

facilitates its conversion to an octahedral state necessary for H_2 coordination. More important is the proton shuttle role of the alcohol in the subsequent heterolytic H_2 cleavage step that is key to forming the 6-membered ring transition state needed to establish a low-barrier reaction path.

Summarizing, the computational results discussed thus far provide an insight into the minimal and essential roles of both the cationic and anionic part of the base in the catalyst activation process. The cation in the reaction scheme considered effectively determines the thermodynamics of the initial Br elimination step by (I) influencing the basicity of the conjugated base and (II) defining the solubility and stability of the resulting bromide salt byproduct. In experiment, the low solubility of the latter would be highly beneficial to achieve its rapid elimination from the reaction mixture. The anionic part of the base plays a more direct role in the current activation scheme. Not only it defines the thermodynamics and kinetics of the intermediate deprotonation steps but also ensures the formation of a favorable reaction environment necessary for a facile hydrogen activation by the deprotonated Mn complex to form the activated Mn-hydrido complex **3**.

3.2. Catalytic cycle

The formation of **3** is the starting point of the ester hydrogenation catalytic cycle. In this section we will discuss the most favorable reaction channels for the initial phase of the ester hydrogenolysis until the formation of an aldehyde intermediate (complex **7** in Scheme 2). The optimized structures of the reaction intermediates and transition states along with the respective energetics of the elementary transformations are presented in Fig. 3. As we will discuss in the next section, aldehyde reduction is a facile process and follows a fundamentally similar mechanism. In this section, the mechanistic analysis will consider the conversion of a model methyl acetate (MeOAc) substrate along the reaction channels that do not directly involve additional promoting reagents except molecular H_2. The mechanistic concepts outlined

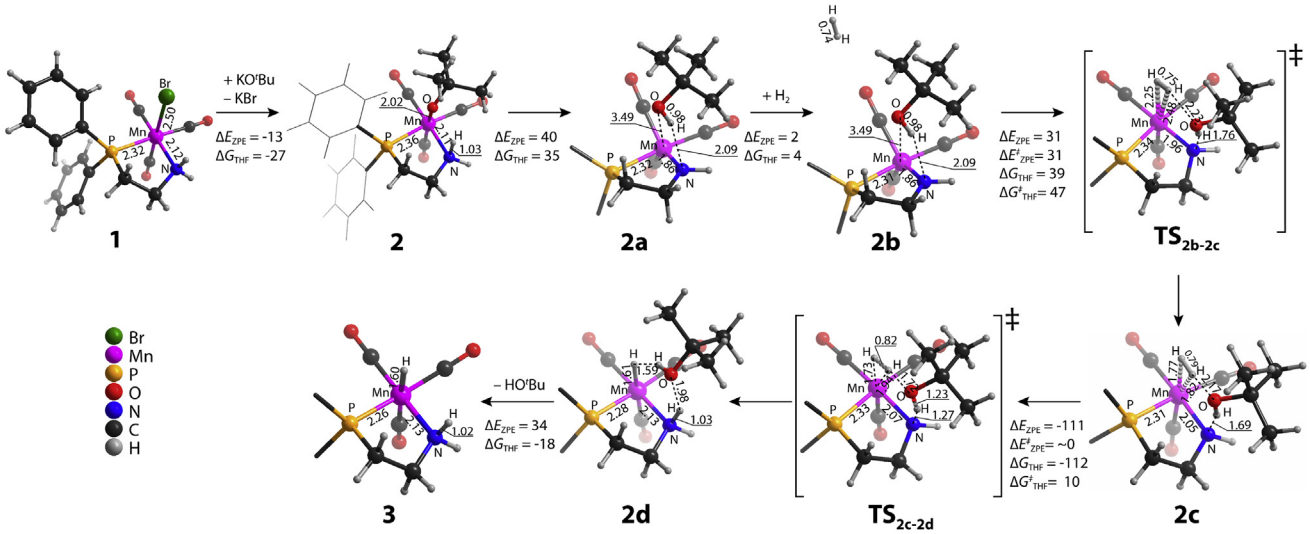

Fig. 1. Optimized structures of reaction intermediates and transition states together with the computed energetics in the preactivation stage of catalyst **1**. ZPE-corrected reaction and activation energies (ΔE_{ZPE} and $\Delta E^{\ddagger}_{ZPE}$), and standard reaction and activation Gibbs free energies (ΔG_{THF} $\Delta G^{\ddagger}_{THF}$) in THF at 373 K are given in kJ mol^{-1}. Bond distances are given in Å.

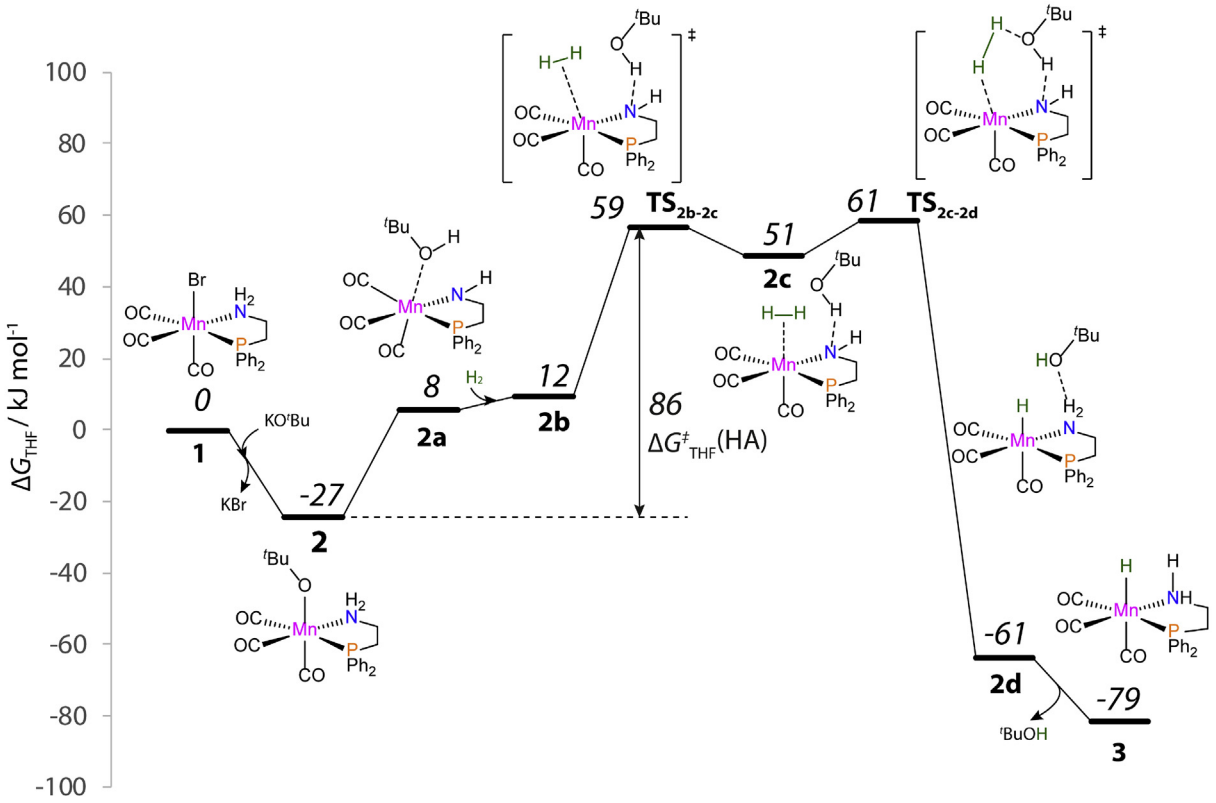

Fig. 2. Standard Gibbs free energy diagrams for the activation of Mn catalyst (THF, 373 K).

here will be used as a basis for the discussion on the catalytic role of the base and the influence of the nature of the substrate in the follow-up sections.

The catalytic reaction starts with a slightly exothermic complexation of **3** with MeOAc to give **3a**. The formation of a hydrogen bond between the carbonyl moiety of the substrate and the NH group of the ligand (r(NH···OC) = 1.96 Å) is the main driving force for the formation of adduct **3a** and it also appears to play a role in defining the subsequent reaction channel. The transfer of the proton along this hydrogen bond effectively increases the electrophilicity of the adjacent carbonyl moiety enabling thus the hydride attack and the conversion of **3a** to **4** via a concerted transition state $\mathbf{TS_{3a-4}}$. Interestingly, our extensive relaxed potential energy scan calculations carried out to establish the most favorable reaction channel for this conversion pointed to the crucial role of the proton transfer at the initial phase of the reduction process. Counterintuitively, the reaction channels initiated by the hydride transfer more often failed to reach the desired product and

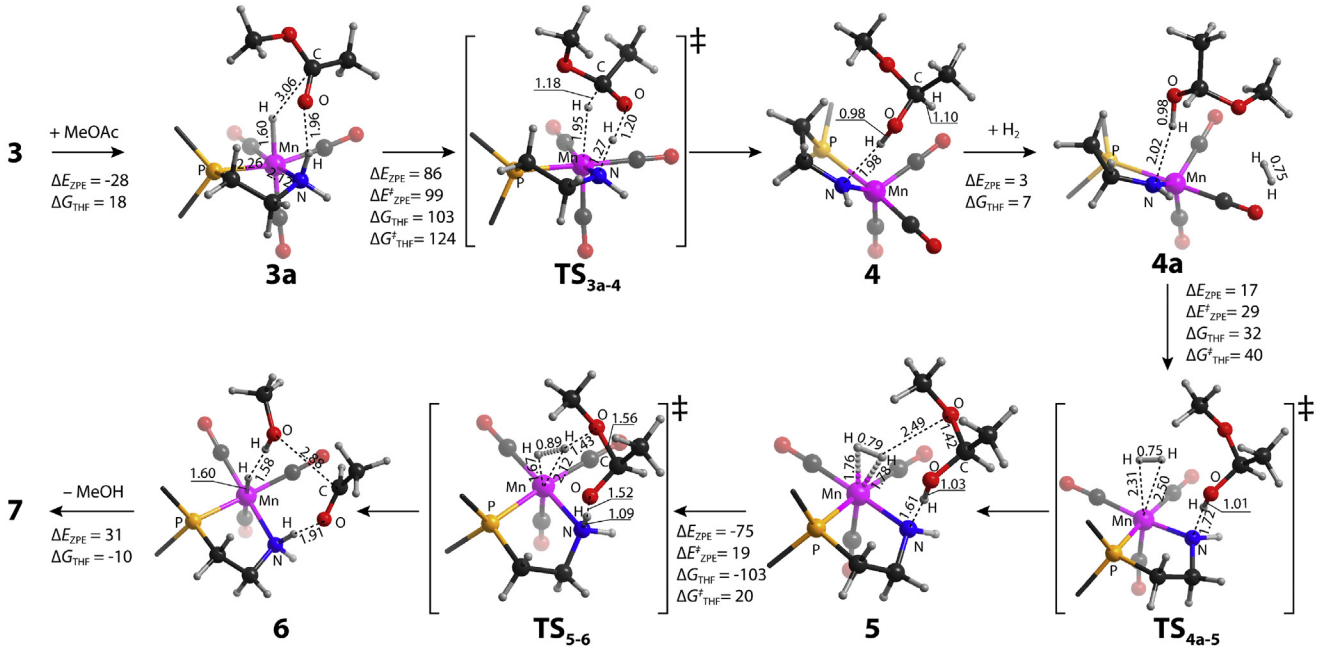

Fig. 3. Elementary reaction steps for MeOAc hydrogenation with **3** to acetaldehyde and methanol. ZPE-corrected reaction and activation energies (ΔE_{ZPE} and $\Delta E^{\ddagger}_{ZPE}$), and standard reaction and activation Gibbs free energies (ΔG_{THF} $\Delta G^{\ddagger}_{THF}$) in THF at 373 K are given in kJ mol^{-1}. Bond distances are given in Å.

commonly showed a more steep energy profile. Nevertheless, even the concerted reduction path to **4** that is an acetal intermediate hydrogen-bonded with the deprotonated Mn-P,N is a highly activated process. The reaction is endergonic by 103 kJ mol^{-1} and shows a free energy barrier of 124 kJ mol^{-1}. It is followed by the coordination of an H_2 molecule (**4** + H_2 → **5**) that further increases the free energy of the system by 39 kJ mol^{-1} and proceeds with an overall barrier of 47 kJ mol^{-1}. Similar to catalyst preactivation process discussed above, these energy losses are partially recovered at the next step involving heterolytic splitting of H_2 (**5** → **6**). In the current catalytic mechanism, the ether moiety of the acetal acts as the proton-accepting base site. This protonation of the acetal intermediate and the formation of a new Mn—H bond are accompanied by the reprotonation of the P,N ligand with a simultaneous cleavage of the C—O bond to yield **6** containing acetaldehyde and methanol products coordinated to the starting Mn—H complex in a single step. Despite the low basicity of the acetal, this step proceeds with a very low barrier of only 20 kJ mol^{-1}. The slightly exergonic elimination of methanol byproduct from **6** gives adduct **7**, from which a facile aldehyde reduction takes place. The computed barrier for acetaldehyde reduction in **7** to ethanol is only 48 kJ mol^{-1} that is almost 3-fold lower than the respective barrier for the ester reduction.

Besides this main reaction channel, our calculations reveal an alternative path that diverges from complex **4** (Fig. 4) and involves the direct decomposition of the acetal intermediate to form a Mn-alkoxide intermediate **4c** and acetaldehyde. The reaction is initiated by the deprotonation of the acetal by the strongly basic amide-moiety of the deprotonated P,N ligand. The formation of the methoxide adduct effectively blocks the catalytic reaction. The free energy diagrams presented in Fig. 5 clearly show that this side-path (**4** → **4b** → **4c**) is much more favorable both kinetically and thermodynamically than the alternative H_2 coordination steps (**4** → **4a** → **5**) providing a plausible explanation for the lack of the catalytic performance of the Mn-P,N catalysts under base-free conditions. The methoxy ligand binds strongly to the Mn center resulting in its lower reactivity towards H_2 activation necessary to proceed with the catalytic conversion. Experimental data shows that the reactivity of the complex can be restored by the addition

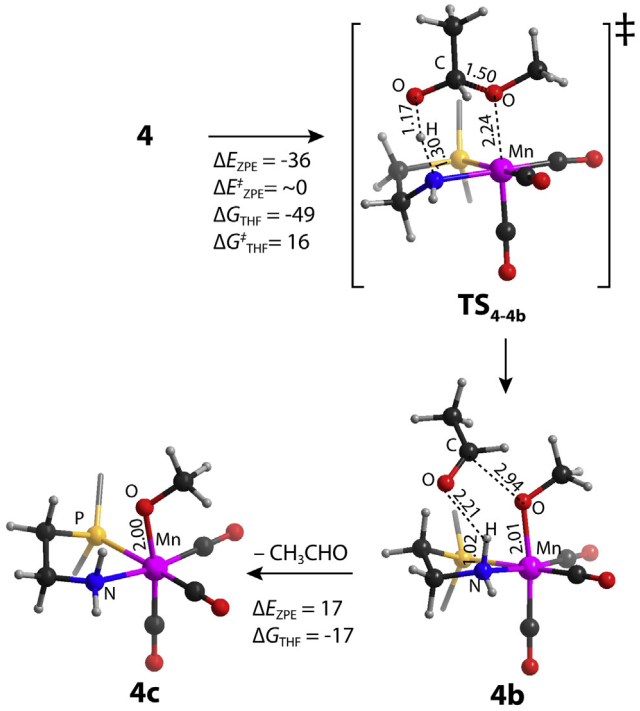

Fig. 4. Transformation of hemiacetal intermediate **4** into Mn-methoxide complex **4c** in resting state. ZPE-corrected reaction and activation energies (ΔE_{ZPE} and $\Delta E^{\ddagger}_{ZPE}$), and standard reaction and activation Gibbs free energies (ΔG_{THF} and $\Delta G^{\ddagger}_{THF}$) in THF solution at 373 K are given in kJ mol^{-1}. Bond distances are given in Å.

of extra KO^{t}Bu base [19], pointing to the crucial role of the base additive in the catalytic hydrogenation.

3.3. Catalytic role of base additive

The results presented thus far suggest that the direct ester reduction with Mn-P,N catalyst following a conventional

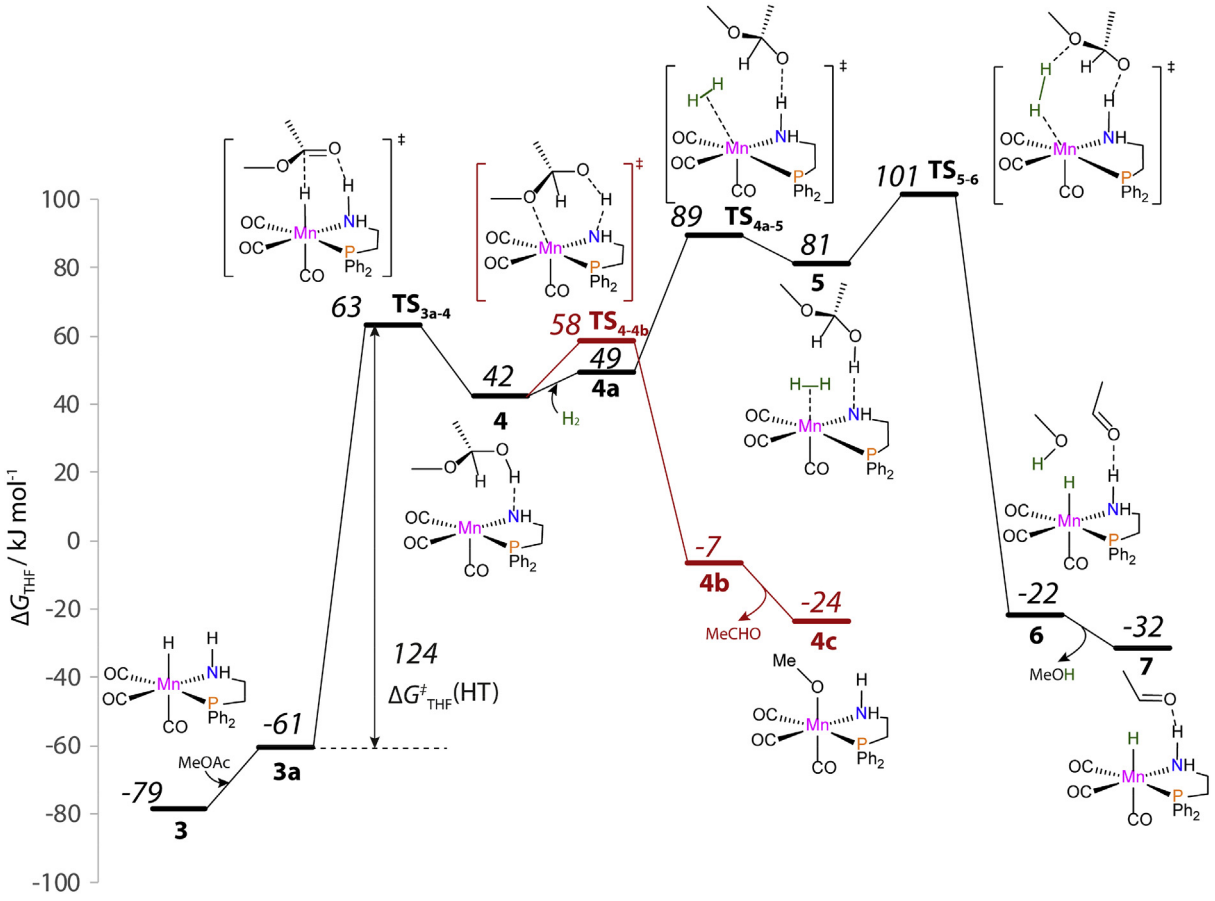

Fig. 5. Standard Gibbs free energy diagrams for catalytic hydrogenation of methyl acetate with Mn catalyst (THF, 373 K).

metal-ligand cooperative mechanism proceeds with an unexpectedly high barrier for the key hydride tranfer step (**3a** → **4**) and is additionally hampered by the formation of a stable alkoxide adducts resting state. These observations suggest a potential dual role of the base for the catalytic mechanism that is (i) the promotion of the hydride transfer and (ii) hydrogenolysis steps. The hydride transfer over **3** requires a prior polarization of the substrate. The "base-free" mechanism implies that such a polarization is achieved through the interaction with a proton generated during the rather unfavorable deprotonation of the NH group of the ligand. The presence of a large and accessible alkali cations of the conjugated alkoxide base additive within the reactive complex could provide the required polarization of the carbonyl group while retaining the stable configuration of the transition metal complex. Heterolytic cleavage of hydrogen over Mn-P,N is crucial for the regeneration of the Mn-H catalytic species both during the catalytic cycle and upon the hydrogenolysis of the alkoxide resting state. Basicity of the proton accepting site effectively controls the reactivity of these steps. The base additive is ultimate proton acceptor in the reaction medium and its reactivity is defined by the nature of its both ionic components [34].

3.3.1. Hydrogenation step

In the presence of strong inorganic bases such as alkali alkoxides (e.g. KO^{t}Bu) commonly employed as the base additives in hydrogenation catalysis, the N-H moiety of the Mn-P,N complex can be replaced by K-N [25,35]. Such a substitution reaction for complex **3** with KO^{t}Bu proceeds with a free energy barrier of 38 kJ mol^{-1} (Fig. S1). To analyze the potential effect of such a substitution, the activation barriers for the hydrogenation of a range of model substrates over complex **3** and its analogue featuring the N-K moiety (**3K**) were compared (Scheme 3).

The computed activation energy and free energy barriers for the respective elementary reaction steps are summarized in Table 1. These results support the hypothesis on the promoting effect of the amide functionality on the hydrogenation step. For all substrates, calculations predict 10–25 kJ mol^{-1} lower barriers over **3K** compared to the parent NH-containing complex **3**. In line with the proposal of Dub and Gordon [24], this promoting effect is mostly related to entropic factors. The secondary interaction with the alkali cation effectively directs the transformation of the activated substrate towards the desirable product. The electronic stabilization via polarization of the carbonyl moiety is most pronounced for the less bulky substrates (e.g. MeCOOMe) that allow for a more efficient interaction with both reactive centers in the complex. The minor role of the electronic polarization is further apparent from the reverse trend of the alkali-promotion with the expected Lewis acidity of the cations. The effect of the nature of the alkali cation was analyzed for the conversion of the most bulky PhCOO^{t}Bu substrate. Although all alkali-modified catalysts showed a strong promoting effect on the free energy profile of the reaction compared to the parent NH form of the catalyst, the variation among the different alkali forms was only minor.

3.3.2. H_2 activation

A conceptually similar promoting effect of alkali cations can be noted for the hydrogen activation step over an alkoxide intermediate (Table 2). The presence of a large and mobile K^+ cation effectively increases the basicity of the MeO^- species resulting in the decrease of the respective barrier for the hydrogenolysis step

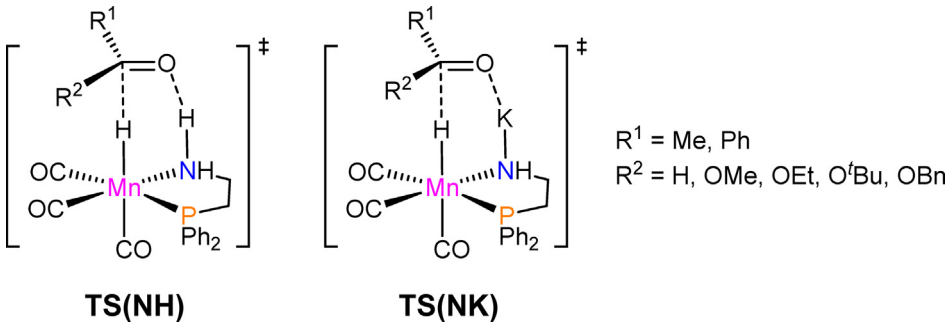

Scheme 3. Schematic representation of the transition states for the hydride transfer step from Mn-hydrido P,N complex to a model carbonyl-containing substrate.

Table 1
Effect of K^+ cations on the reaction barriers of ester hydrogenation (HT) step.

Substrate	TS(NH)		TS(NK)	
	$\Delta E^{\neq}_{ZPE}$	$\Delta G^{\neq}_{THF}$	$\Delta E^{\neq}_{ZPE}$	$\Delta G^{\neq}_{THF}$
MeCOOMe	99	124	85	100
PhCOOMe	99	126	101	114
PhCOOEt	97	117	95	108
PhCOO^{t}Bu*	109	141	104	125
PhCOOBn	94	118	88	104
MeCHO	31	48	24	33
PhCHO	39	55	28	50

* $\Delta E^{\neq}_{ZPE}$ and $\Delta G^{\neq}_{THF}$ for TS(NLi) are 111 and 128 kJ mol^{-1}; for TS(NNa) are 106 and 124 kJ mol^{-1}, respectively.

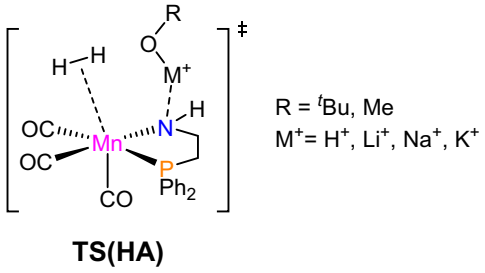

Scheme 4. Schematic representation of the transition state for the alkoxyde hydrogenolysis/hydrogen activation (HA) step.

(Scheme 4) by ca. 10 kJ mol^{-1} compared to the NH-form of the catalyst. However, this promoting effect of the alkali cations is quite minor and cannot provide a sufficient driving force for the recovery of the catalytic complex from the alkoxide resting state. To enable the catalytic conversion of the ester, the small and strongly-bound MeO^- species needs to be exchanged for a bulkier and more mobile $^tBuO^-$ present in a high concentration in the working catalytic system. The combination of the K^+ with $^tBuO^-$ in the base promotor allows decreasing the free energy barrier for the hydrogenolysis of the alkoxide by more than 30 kJ mol^{-1} (Table 2).

We further performed a thermodynamic analysis using realistic solvent models the Conductor-like Screening Model for Real Solvents (COSMO-RS) [36,37] and corrected the free energies for varying base concentration (for details see the supporting information). The computed concentration-dependent free energy changes for the key elementary steps at the reaction conditions (373 K, 50 bar H_2) are shown in Fig. 6. The data confirms generally the discussion above based on the standard enthalpies and Gibbs free energies. Only in the presence of an external base the hydrogenolysis of the methoxide adduct (**4c** + H_2 → **3** + MeOH) becomes thermodynamically favorable. However, the base assisted path involving the alkoxide exchange step to form a *tert*-butoxide adduct (**4c** + KO^{t}Bu → **2** + KOMe) followed by its hydrogenolysis (**2** + H_2 → **3** + ^{t}BuOH) is much more exergonic at all conditions. The concentration-dependent free energy profiles presented in Fig. 6 indicate that the base not only acts as a reagent in the conversions discussed here but it also (at least at high concentrations) acts as a solvent affecting thus nonlinearly the energetics of the elementary steps.

Table 2
Effect of alkali metal cations on the reaction barriers of H_2 activation (HA).

Cation	R = ^{t}Bu		R = Me	
	$\Delta E^{\neq}_{ZPE}$	$\Delta G^{\neq}_{THF}$	$\Delta E^{\neq}_{ZPE}$	$\Delta G^{\neq}_{THF}$
H^+	72	86	91	106
Li^+	66	84	85	101
Na^+	67	85	88	105
K^+	65	73	91	95

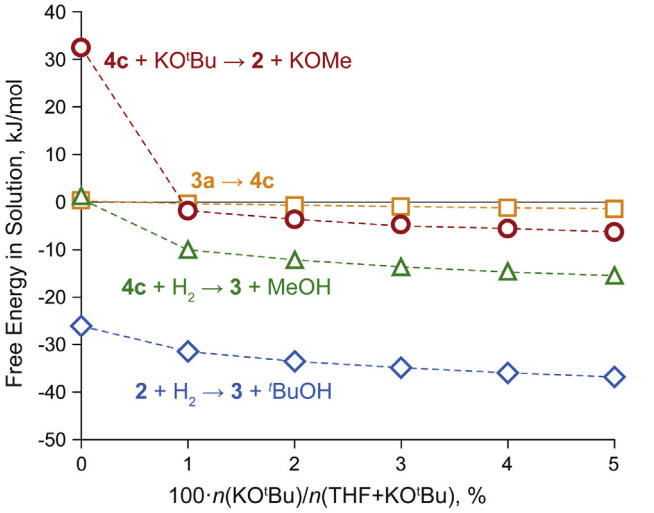

Fig. 6. Concentration-dependent free energy changes for the key elementary steps at the reaction conditions (373 K, 50 bar H_2) computed using a realistic COSMO-RS solvent model.

4. Conclusion

The reaction mechanism of ester hydrogenation catalyzed by a bidentate aminophosphine ligated manganese catalyst in the presence of inorganic alkoxide bases was studied by DFT calculations. Calculations reveal that besides the direct involvement of KO^{t}Bu as the stoichiometric reagent during the pre-catalyst activation, the inorganic base plays an important role in the catalytic cycle. We propose that the secondary interactions of the carbonyl moiety

with a hard Lewis acidic K^+ cations within the catalytic complex pre-activate the substrate and facilitate substantially the key hydride-transfer step of the catalytic ester reduction. The direct accessibility and pronounced mobility of the large potassium cations is shown to be more important for this process than its polarizing power that is the Lewis acidity. The promotion effect is most apparent from the variation of the activation free energy rather than its electronic counterpart indicating the crucial role of the entropic factors for the hydride transfer step. Furthermore, the presence of the inorganic base in the reaction mixture promotes the hydrogen activation steps required for the regeneration of the catalytic Mn-hydrido complexes. The DFT calculations reveal that the main catalytic cycle over the Mn-P,N catalyst operates via the outer-sphere mechanism. A competing path resulting in the formation of stable Mn-alkoxide intermediates is identified and it results in the in situ catalyst inhibition. The reaction with a strong inorganic base facilitates the hydrogenolysis of such a resting state intermediate to reactivate the catalytic system. For this process, the bulkiness of the anionic part and, accordingly, the mobility of the alkoxide moiety is the primary factor determining the reactivity.

Acknowledgments

This project has received funding from the European Research Council (ERC) under the European Union's Horizon 2020 research and innovation programme (grant agreement No. 725686). P.O.K. acknowledges the partial support from the Government of the Russian Federation (Grant 08-08) and the Ministry of Education and Science of Russian Federation (Project 11.1706.2017/4.6). The authors thank the Netherlands Organization for Scientific Research (NWO) for the access to SurfSARA computational facilities.

Appendix A. Supplementary material

Supplementary data associated with this article can be found, in the online version, at https://doi.org/10.1016/j.jcat.2018.04.018.

References

[1] A.M. Smith, R. Whyman, Review of methods for the catalytic hydrogenation of carboxamides, Chem. Rev. 114 (2014) 5477–5510.
[2] B. Chen, U. Dingerdissen, J.G.E. Krauter, H.G.J. Lansink Rotgerink, K. Moebus, D. J. Ostgard, P. Panster, T.H. Riermeier, S. Seebald, T. Tacke, H. Trauthwein, New developments in hydrogenation catalysis particularly in synthesis of fine and intermediate chemicals, Appl. Catal., A 280 (2005) 17–46.
[3] J. Pritchard, G.A. Filonenko, R. van Putten, E.J.M. Hensen, E.A. Pidko, Heterogeneous and homogeneous catalysis for the hydrogenation of carboxylic acid derivatives: history, advances and future directions, Chem. Soc. Rev. 44 (2015) 3808–3833.
[4] D. Wang, D. Astruc, The golden age of transfer hydrogenation, Chem. Rev. 115 (2015) 6621–6686.
[5] C. Hu, D. Creaser, S. Siahrostami, H. Groenbeck, H. Ojagh, M. Skoglundh, Catalytic hydrogenation of C=C and C=O in unsaturated fatty acid methyl esters, Catal. Sci. Technol. 4 (2014) 2427–2444.
[6] J. Magano, J.R. Dunetz, Large-scale carbonyl reductions in the pharmaceutical industry, Org. Proc. Res. Dev. 16 (2012) 1156–1184.
[7] L.C. Misal Castro, H. Li, J.-B. Sortais, C. Darcel, When iron met phosphines: a happy marriage for reduction catalysis, Green Chem. 17 (2015) 2283–2303.
[8] G. Bauer, X. Hu, Recent developments of iron pincer complexes for catalytic applications, Inorg. Chem. Front. 3 (2016) 741–765.
[9] J.-L. Renaud, S. Gaillard, Recent advances in iron- and cobalt-complex-catalyzed tandem/consecutive processes involving hydrogenation, Synthesis 48 (2016) 3659–3683.
[10] J. Yuwen, S. Chakraborty, W.W. Brennessel, W.D. Jones, Additive-free cobalt-catalyzed hydrogenation of esters to alcohols, ACS Catal. 7 (2017) 3735–3740.
[11] T.J. Korstanje, J. Ivar van der Vlugt, C.J. Elsevier, B. de Bruin, Hydrogenation of carboxylic acids with a homogeneous cobalt catalyst, Science 350 (2015) 298–302.
[12] G.A. Filonenko, R. van Putten, E.J.M. Hensen, E.A. Pidko, Catalytic (de) hydrogenation promoted by non-precious metals - Co, Fe and Mn: recent advances in an emerging field, Chem. Soc. Rev. 47 (2018) 1459–1483.
[13] F. Kallmeier, R. Kempe, Manganese complexes for (De)hydrogenation catalysis: a comparison to cobalt and iron catalysts, Angew. Chem. Int. Ed. 57 (2018) 46–60.
[14] J.R. Carney, B.R. Dillon, S.P. Thomas, Recent advances of manganese catalysis for organic synthesis, Eur. J. Org. Chem. 2016 (2016) 3912–3929.
[15] B. Maji, M.K. Barman, Recent developments of manganese complexes for catalytic hydrogenation and dehydrogenation reactions, Synthesis 49 (2017) 3377–3393.
[16] J.R. Khusnutdinova, D. Milstein, Metal-ligand cooperation, Angew. Chem. Int. Ed. 54 (2015) 12236–12273.
[17] T. Zell, D. Milstein, Hydrogenation and dehydrogenation iron pincer catalysts capable of metal-ligand cooperation by aromatization/dearomatization, Acc. Chem. Res. 48 (2015) 1979–1994.
[18] D.H. Nguyen, X. Trivelli, F. Capet, J.-F. Paul, F. Dumeignil, R.M. Gauvin, Manganese pincer complexes for the base-free, acceptorless dehydrogenative coupling of alcohols to esters: development, scope, and understanding, ACS Catal. 7 (2017) 2022–2032.
[19] R. van Putten, E.A. Uslamin, M. Garbe, C. Liu, A. Gonzalez-de-Castro, M. Lutz, K. Junge, E.J.M. Hensen, M. Beller, L. Lefort, E.A. Pidko, Non-pincer-type manganese complexes as efficient catalysts for the hydrogenation of esters, Angew. Chem. Int. Ed. 56 (2017) 7531–7534.
[20] R.J. Hamilton, S.H. Bergens, An unexpected possible role of base in asymmetric catalytic hydrogenations of ketones. Synthesis and characterization of several key catalytic intermediates, J. Am. Chem. Soc. 128 (2006) 13700–13701.
[21] K. Abdur-Rashid, S.E. Clapham, A. Hadzovic, J.N. Harvey, A.J. Lough, R.H. Morris, Mechanism of the hydrogenation of ketones catalyzed by trans-dihydrido (diamine)ruthenium(II) complexes, J. Am. Chem. Soc. 124 (2002) 15104–15118.
[22] R. Hartmann, P. Chen, Noyori's hydrogenation catalyst needs a lewis acid cocatalyst for high activity, Angew. Chem. Int. Ed. 40 (2001) 3581–3585.
[23] W.H. Bernskoetter, N. Hazari, Reversible hydrogenation of carbon dioxide to formic acid and methanol: lewis acid enhancement of base metal catalysts, Acc. Chem. Res. 50 (2017) 1049–1058.
[24] P.A. Dub, J.C. Gordon, Metal–Ligand Bifunctional Catalysis: The "Accepted" Mechanism, the Issue of Concertedness, and the Function of the Ligand in Catalytic Cycles Involving Hydrogen Atoms, ACS Catal., 7 (2017) pp. 6635–6655.
[25] P.A. Dub, N.J. Henson, R.L. Martin, J.C. Gordon, Unravelling the mechanism of the asymmetric hydrogenation of acetophenone by [RuX2(diphosphine)(1,2-diamine)] Catalysts, J. Am. Chem. Soc. 136 (2014) 3505–3521.
[26] P.A. Dub, B.L. Scott, J.C. Gordon, Why does alkylation of the N-H functionality within M/NH bifunctional Noyori-type catalysts lead to turnover?, J Am. Chem. Soc. 139 (2017) 1245–1260.
[27] C. Adamo, V. Barone, Toward reliable density functional methods without adjustable parameters: The PBE0 model, J. Chem. Phys. 110 (1999) 6158–6170.
[28] Gaussian 09 Rev. D.01, M.J. Frisch, G.W. Trucks, H.B. Schlegel, G.E. Scuseria, M. A. Robb, J.R. Cheeseman, G. Scalmani, V. Barone, B. Mennucci, G.A. Petersson, H. Nakatsuji, M. Caricato, X. Li, H.P. Hratchian, A.F. Izmaylov, J. Bloino, G. Zheng, J. L. Sonnenberg, M. Hada, M. Ehara, K. Toyota, R. Fukuda, J. Hasegawa, M. Ishida, T. Nakajima, Y. Honda, O. Kitao, H. Nakai, T. Vreven, J.A. Montgomery Jr., J.E. Peralta, F. Ogliaro, M. Bearpark, J.J. Heyd, E. Brothers, K.N. Kudin, V.N. Staroverov, R. Kobayashi, J. Normand, K. Raghavachari, A. Rendell, J.C. Burant, S.S. Iyengar, J. Tomasi, M. Cossi, N. Rega, N.J. Millam, M. Klene, J.E. Knox, J.B. Cross, V. Bakken, C. Adamo, J. Jaramillo, R. Gomperts, R.E. Stratmann, O. Yazyev, A.J. Austin, R. Cammi, C. Pomelli, J.W. Ochterski, R.L. Martin, K. Morokuma, V.G. Zakrzewski, G.A. Voth, P. Salvador, J.J. Dannenberg, S. Dapprich, A.D. Daniels, Ö. Farkas, J.B. Foresman, J.V. Ortiz, J. Cioslowski, D.J. Fox, Gaussian, Inc., Wallingford CT, 2009.
[29] G.A. Filonenko, D. Smykowski, B.M. Szyja, G. Li, J. Szczygieł, E.J.M. Hensen, E.A. Pidko, Catalytic hydrogenation of CO2 to formates by a lutidine-derived Ru–CNC pincer complex: theoretical insight into the unrealized potential, ACS Catal. 5 (2015) 1145–1154.
[30] G.A. Filonenko, E.J.M. Hensen, E.A. Pidko, Mechanism of CO_2 hydrogenation to formates by homogeneous Ru-PNP pincer catalyst: from a theoretical description to performance optimization, Catal. Sci. Technol. 4 (2014) 3474–3485.
[31] J.A. Gámez, M. Hölscher, W. Leitner, On the applicability of density functional theory to manganese-based complexes with catalytic activity toward water oxidation, J. Comp. Chem. 38 (2017) 1747–1751.
[32] D.V. Deubel, J.K.-C. Lau, In silico evolution of substrate selectivity: comparison of organometallic ruthenium complexes with the anticancer drug cisplatin, Chem. Commun. 2451–2453 (2006).
[33] J. Kua, A.A. Rodriguez, L.A. Marucci, M.M. Galloway, D.O. De Haan, Free energy map for the co-oligomerization of formaldehyde and ammonia, J. Phys. Chem. A 119 (2015) 2122–2131.
[34] N.V. Belkova, O.A. Filippov, E.S. Shubina, Z–H bond activation in (Di)hydrogen bonding as a way to proton/hydride transfer and H_2 evolution, Chem. Eur. J. 24 (2018) 1464–1470.
[35] J.M. John, S. Takebayashi, N. Dabral, M. Miskolzie, S.H. Bergens, Base-catalyzed bifunctional addition to amides and imides at low temperature. A new pathway for carbonyl hydrogenation, J. Am. Chem. Soc. 135 (2013) 8578–8584.
[36] A. Klamt, Conductor-like screening model for real solvents: a new approach to the quantitative calculation of solvation phenomena, J. Phys. Chem. 99 (1995) 2224–2235.
[37] A. Klamt, V. Jonas, T. Bürger, J.C.W. Lohrenz, Refinement and parametrization of COSMO-RS, J. Phys. Chem. A 102 (1998) 5074–5085.